

A statistical model for predicting thermal chemical reaction rate*

Lin Zheng-Zhe(林正喆)^{a)}, Li Wang-Yao(李王尧)^{b)c)}, and Ning Xi-Jing(宁西京)^{a)†}

^{a)}Institute of Modern Physics, Department of Nuclear Science and Technology, Fudan University, Shanghai 200433, China

^{b)}Department of Physics, Fudan University, Shanghai 200433, China

^{c)}State Key Laboratory of Surface Physics, Fudan University, Shanghai 200433, China

(Received 24 August 2013; revised manuscript received 7 November 2013; published online 25 March 2014)

A simple model based on the statistics of individual atoms [*Europhys. Lett.* **94** 40002 (2011)] or molecules [*Chin. Phys. Lett.* **29** 080504 (2012)] was used to predict chemical reaction rates without empirical parameters, and its physical basis was further investigated both theoretically and via MD simulations. The model was successfully applied to some reactions of extensive experimental data, showing that the model is significantly better than the conventional transition state theory. It is worth noting that the prediction of the model on *ab initio* level is much easier than the transition state theory or unimolecular RRKM theory.

Keywords: chemical reaction rate, transition state theory, unimolecular reaction, bimolecular reaction

PACS: 05.20.Dd, 34.50.Lf, 71.15.Pd

DOI: 10.1088/1674-1056/23/5/050501

1. Introduction

In the design of molecules and material, theoretical models are highly desired to precisely predict the rate of various chemical reactions in thermal environment. Obviously, the model should be accurate enough without the help of empirical parameters, and work in a uniform (or unique) way rather than changing its operation for different reactions. Furthermore, it should be simple enough to work on the *ab initio* level. Bearing this in mind, we first briefly examine the common used models for predicting the reaction rate.

In 1889, Arrhenius experimentally summarized a simple law on reaction rate constant k changing with reaction temperature T

$$k = A e^{-E_a/k_B T}, \quad (1)$$

where A and E_a are two parameters to be determined experimentally. From then on, the Arrhenius law was applied not only to elementary chemical reaction but also to the atomic diffusion on surfaces^[1] or in materials,^[2] the failure of polymers,^[3] the creep of metallic materials, and so on. However, experiments show that some reactions are obviously non-Arrhenius,^[4] and the parameter A and E_a can hardly be determined without empirical data because their physical sense is not well understood.^[1,4,5]

In 1918, Lewis suggested a simple collision theory to describe the second-order rate constant of bimolecular reactions

$$k_{2nd} = \delta_{AB} \sqrt{\frac{8k_B T}{\pi\mu}} e^{-E_c/k_B T}, \quad (2)$$

where δ_{AB} was proposed to be the effective molecular cross-section corresponding to specific geometry of the potential

surface, and E_c defined as the collision threshold energy is closely relevant not only to the static potential barrier but also to the innermolecular states. However, many experimental results do not comply with this rule. Modern molecular reaction kinetics measurements go into the details of molecular collisions and reactions, and reveal that δ_{AB} and E_c are not constants but dependent on molecular quantum states, orientations and temperatures, leading to a too complicated model to work in practice.

As the first modeling reaction rate theory, the transition state theory (TST) developed in 1935 gives the expression for the rate constant^[6–8]

$$k = \frac{k_B T}{h} \frac{Q_{TS}}{Q_{react}} e^{-E_0/k_B T}, \quad (3)$$

where E_0 is the static potential barrier along the MEP, while Q_{TS} and Q_{react} are the total partition functions for the transition configuration and the whole system (reactant), respectively. By taking the whole system as a quantum statistical model, the partition functions Q_{TS} and Q_{react} are not easy to be precisely evaluated because the potential surface is usually not of simple shape. Thus, empirical information such as spectroscopic data is used to evaluate Q_{react} ,^[4] and some over-simple approximations, such as the rigid rotor harmonic oscillator approximation together with empirical corrections to avoid numerical errors for the canonical frequencies, have to be resorted in current *ab initio* schemes.

In principle, for reactions with relatively smaller E_0 , the TST expression (3) may overestimates the rate constant due to ignorance of the re-crossing effect. Hence, several advanced versions of the TST, e.g., canonical variation TST,

*Project supported by the National Natural Science Foundation of China (Grant No. 11274073) and the Leading Academic Discipline Project of Shanghai, China (Grant No. B107).

†Corresponding author. E-mail: xjning@fudan.edu.cn

the microcanonical TST and the statistical adiabatic channel model,^[7,9–11] have been proposed, and recently, a resolved version of the variation TST was implemented.^[12] However, such improvements need to find a dividing surface on the total potential surface, which is quite difficult for *ab initio* calculations. For reactions with relatively larger E_0 (or reactions at low temperature), quantum effects should be taken into account, and nuclear quantum effects were considered in experiments such as the enzymatic reactions at physiological temperatures^[13,14] or organic reactions^[15,16] at very low temperatures. Very recently, semiclassical methods,^[17,18] the quantum TST,^[19–21] or quantum instanton approximation^[22] were used to address the issue. In addition, novel approaches beyond the TST, such as ring polymer molecular dynamics,^[23–25] were developed.

In spite of the significant development of the TST, obvious deviations are frequently observed in various experiments,^[13,14] and sometimes, the deviation in reaction rate may be as large as an order of magnitude even at high temperature where quantum effects can be ignored. Similar problems also appear in other rate theories, such as the RRKM theory^[26] for unimolecular reactions and modern molecular reaction kinetics for bimolecular reactions. In such situations, although most experimental data can be eventually understood theoretically by selecting different theoretical methods, the theoretical ability for designing new molecules and materials is seriously reduced because of the absence of uniform theoretical model for different reaction systems.

At the atomistic level, most elementary reaction processes concern only one or two atoms, namely “key atoms”, and the other atoms can be equivalent to providing a mean potential for motion of the key atoms. From this point of view, a statistical mechanical model was developed to calculate thermal reaction rates without empirical parameters, and has been successfully applied on predicting the bond breaking rates of monatomic chains.^[27] In the present work, the same model was applied to elementary chemical reactions $\text{CH}_4 \rightarrow \text{CH}_3 + \text{H}$, $\text{CH}_3\text{OH} \rightarrow \text{CH}_3 + \text{OH}$, and $\text{CF}_3\text{CH}_2\text{Cl} \rightarrow \text{CF}_2\text{CHCl} + \text{HF}$. These specific reactions were selected since there were extensive experimental data on the reaction rate versus temperature. It is shown that our model is obviously better than the TST, especially, the potential barrier E_0 drawn from the TST fitting to the experimental data is obviously lower than the values determined by other experimental methods. In order to strictly test our model further, molecular dynamics (MD) simulations were performed on the Stone–Wales transformation of a C_{60} molecule, and the results are in excellent agreement with the model but far from the prediction of the TST.

2. Theoretical model

For the motion of free molecules at room temperature or above, the thermal De Broglie wavelength of molecular mass center is of the magnitude of 0.01 Å, which is about 100 times smaller than the molecular size, so the quantum state density of thermal molecules approaches to continuum and the motion of molecular mass center can be understood in classical pictures. For the atoms bounded in molecules, the kinetic energy distribution is determined by $f(\varepsilon) = \sum_i f_i(\varepsilon) e^{-E_i/k_B T} / \sum_i e^{-E_i/k_B T}$, where $f_i(\varepsilon)$ is the kinetic energy distribution of quantum state E_i , including all of the translational, rotational, and vibrational states, and when the temperature rises to a critical temperature T_c , and the distribution $f(\varepsilon)$ turns into a classical one. For an O_2 molecule (with a Debye temperature $T_D = 2278$ K), the atomic kinetic energy distribution gets close to a classical Boltzmann distribution when the temperature is higher than $T_c = 1000$ K, i.e., $0.44T_D$ (see Fig. 1(a)). For polyatomic molecules, the vibrational modes invoking unimolecular reactions are always with lower Debye temperatures, and the corresponding T_c should be lower. In solid materials, the atomic motions should be more classical due to an amount of near-continual vibrational states.

In the classical limit, the Boltzmann kinetic energy distribution $\varepsilon^{1/2} e^{-\varepsilon/k_B T}$ for individual atoms in the molecule can be easily derived from classical ensemble theory. For a classical mechanical system including N atoms, the total energy $E = \mathbf{p}_1^2/2m_1 + \dots + \mathbf{p}_N^2/2m_N + V(\mathbf{x}_1, \dots, \mathbf{x}_N)$ and the kinetic energy distribution of the i th atom reads

$$\begin{aligned} f(\varepsilon) &= \int \delta[\mathbf{p}_i^2/2m_i - \varepsilon] e^{-E/k_B T} d\mathbf{p}_1 \dots d\mathbf{p}_N d\mathbf{x}_1 \dots d\mathbf{x}_N \\ &\quad / \int \int e^{-E/k_B T} d\mathbf{p}_1 \dots d\mathbf{p}_N d\mathbf{x}_1 \dots d\mathbf{x}_N \\ &= \int \delta[\mathbf{p}_i^2/2m_i - \varepsilon] e^{-\mathbf{p}_i^2/2m_i k_B T} d\mathbf{p}_i / \int e^{-\mathbf{p}_i^2/2m_i k_B T} d\mathbf{p}_i \\ &= \varepsilon^{1/2} e^{-\varepsilon/k_B T} / Z, \end{aligned} \quad (4)$$

where $Z = \sqrt{\pi}(kT)^{3/2}/2$ is the partition function. This distribution is in very good agreement with various MD simulations.^[27] As an example, figure 1(b) shows the kinetic energy distribution of an individual atom in the Pt_5 cluster drawn from the MD simulation of the cluster gas at 100 atm and 300 K by the Tight–Binding potential,^[28] which converges at the Boltzmann distribution in a sampling duration of 100 ps. It should be noted that for dilute gas with a pressure lower than 0.1 atm, the kinetic energy deviates from the Boltzmann distribution (see Fig. 1(c)), which concerns the second-order reaction at low pressures and will be explained below.

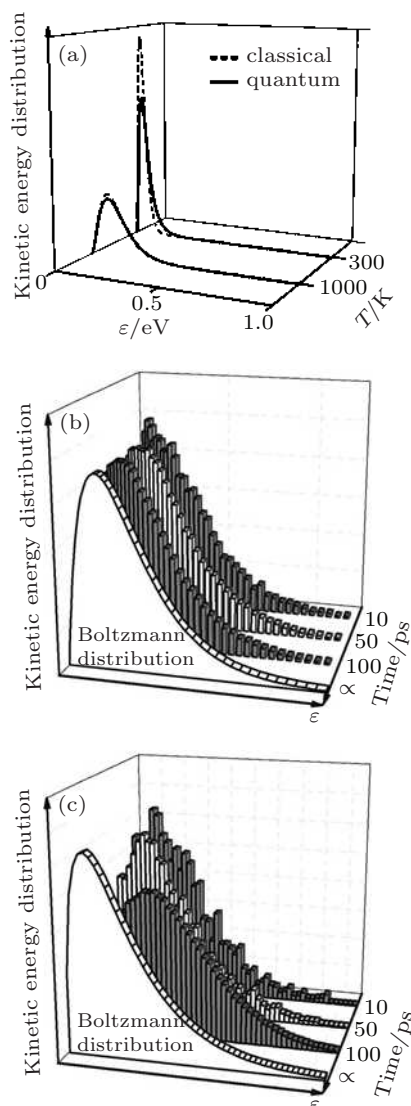


Fig. 1. The kinetic energy distribution of an atom in O_2 molecule by classical (gray dashes) and quantum mechanics (black lines) at 300 and 1000 K (a), and the distribution for an atom of cluster Pt_5 in the cluster gas at 300 K for 100 atm (b) and 0.1 atm (c).

For unimolecular reactions including either reconstruction or dissociation, the significant changing corresponds to some individual atomic events that one or two “key atoms” cross over a barrier E_0 . In most cases, the atomic kinetic energy ($\sim k_B T$) is significantly smaller than E_0 , and the key atom vibrates many times with a frequency Γ_0 in the valley before crossing over the barrier. From this point of view, the first-order thermal reaction rates can be evaluated by^[27]

$$k_{1st} = \frac{\Gamma_0}{Z} \int_{E_0}^{+\infty} \varepsilon^{1/2} e^{-\varepsilon/k_B T} d\varepsilon. \quad (5)$$

Here, Γ_0 can be evaluated by a classical trajectory method. For given energy ε , the atomic oscillation period $\tau(\varepsilon) = \sqrt{m} \int dx / 2[\varepsilon - V(x)]$ can be determined by the potential $V(x)$ felt by the key atom along the minimum energy path

(MEP), and the averaged frequency reads

$$\Gamma_0 = \frac{\int_0^{E_0} v(\varepsilon) \varepsilon^{1/2} e^{-\varepsilon/k_B T} d\varepsilon}{\int_0^{E_0} \varepsilon^{1/2} e^{-\varepsilon/k_B T} d\varepsilon}, \quad (6)$$

where $v(\varepsilon) = 1/\tau(\varepsilon)$.

The above analysis can be tested by MD simulations. As shown in Fig. 2(a), the trajectory of an individual atom in C_{60} fullerene drawn from MD simulation at 300 K^[29] seems irregular, while the relative displacement in the direction of bond stretch presents some periodic behavior (see Fig. 2(b)). It is worth noting that $\Gamma_0(T)$ given by Eq. (6) is in good agreement with the value observed in MD simulations. For example, the frequency obtained by Eq. (6) for the bond stretch mode in C_{60} fullerene is about 2.3×10^{13} Hz at 300 K, which is very close to that drawn from the MD simulation (2.5×10^{13} Hz). This fact has been confirmed by other examples, e.g., the adatom self-diffusion on Cu and Pt surfaces,^[30] in which MD simulations were performed for adatom and dimer self-diffusion by hopping or exchanging on Cu (100), Pt (111) surfaces, and the validity of Eq. (4) was proved.

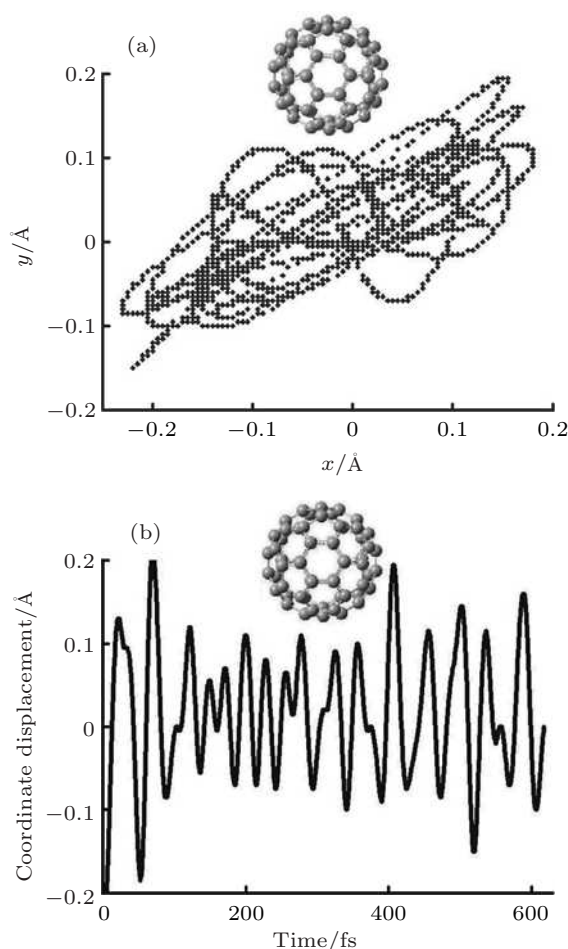


Fig. 2. The thermal motion trajectory of an individual atom in a C_{60} fullerene at 300 K (a) and the corresponding displacement in the bond stretching direction (b).

For a reaction involving two key atoms, the reaction occurs when the kinetic energy plus of the two key atoms $\varepsilon_1 + \varepsilon_2$ is larger than E_0 , and therefore the rate constant should be^[27]

$$k_{1st} = \frac{\Gamma_0}{Z^2} \iint_{\varepsilon_1 + \varepsilon_2 > E_0} \varepsilon_1^{1/2} \varepsilon_2^{1/2} e^{-(\varepsilon_1 + \varepsilon_2)/k_B T} d\varepsilon_1 d\varepsilon_2. \quad (7)$$

It should be noted that quick intermolecular collisions, which correspond to a higher spatial density of molecules, is the necessary condition for kinetic energy distribution $\varepsilon^{1/2} e^{-\varepsilon/k_B T}$. For reactions at lower density, generally a pressure lower than 1 atm, the average period for one molecule colliding with any others is usually longer than 100 ns, which is much longer than the time for one innermolecular vibration. Thus, it cannot be expected that the atomic kinetic energy distribution is still the Boltzmann. As an example, for Pt₅ cluster gas at 0.1 atm and 300 K, the mean time for single cluster freely flying is about 1000 ps, and the kinetic energy distribution (see Fig. 1(c)) drawn from MD simulation in a sampling duration of 100 ps obviously differs from the Boltzmann distribution. In such cases, equation (5) or (7) is no longer applicable, and therefore, the reaction should show a second-order behavior because the rate should be proportional to the intermolecular collision frequency.

For bimolecular reactions due to the collisions of two reactant molecules, A and B with mass m_A and m_B , the reaction occurs when the molecules cross over the potential barrier E_0 . Considering the distribution of relative translational energy is still of Boltzmann kind, the reaction probability of once collision should be

$$P = \frac{1}{Z} \int_{E_0}^{+\infty} \varepsilon^{1/2} e^{-\varepsilon/k_B T} d\varepsilon. \quad (8)$$

A more complicated expression can be deduced from another point of view. The reaction occurs when the kinetic energy sum of the two molecules is larger than E_0 , so the reaction probability reads

$$P = \frac{1}{Z^2} \iint_{\varepsilon_1 + \varepsilon_2 \geq E_0} \varepsilon_1^{1/2} \varepsilon_2^{1/2} e^{-(\varepsilon_1 + \varepsilon_2)/k_B T} d\varepsilon_1 d\varepsilon_2, \quad (9)$$

and the rate constant of the collision reaction should be^[31]

$$k_{2nd} = P\sigma \sqrt{\frac{8k_B T m_A m_B}{\pi(m_A + m_B)}}, \quad (10)$$

where σ is the effective cross-section and can be easily calculated by^[31]

$$\sigma = \frac{\Omega_A \Omega_B}{(4\pi)^2} \pi(R_A + r_A + R_B + r_B)^2, \quad (11)$$

where R_A and R_B are the distances between the key atoms and the mass center of the reactant molecules, and Ω_A (or Ω_B) the solid angle opened by the key atom in A (or B) with a radius of r_A (or r_B) to the molecular mass center.

3. Application to unimolecular reactions

In order to strictly test our model and make comparison with the TST, we perform MD simulations for Stone–Wales transformation of C₆₀ fullerene and consider three elementary unimolecular reactions



These reactions were chosen because the reaction rates were measured in a wide range of temperature,^[32–34] providing precise data to verify our model. Moreover, all the potential barriers E_0 s have been determined accurately by other experimental methods,^[35–37] such as multi-photon absorption for bond dissociation. It should be mentioned that the available experimental data of E_0 are vital for testing the model because usual *ab initio* calculations cannot produce the accurate ones. In fact, classical MD simulations can provide more accurate and credible data for testing the model, because the reaction barrier E_0 can be exactly determined by the interaction potential function and the reaction rate can be well determined by counting the reaction events one by one at femtosecond interval. More importantly, no quantum effect takes place in classical MD simulations and every rate theory can be exactly examined at a pure classical level. Here, the Stone–Wales transformation of C₆₀ fullerene was employed as a typical example. The simulation system was set up by putting a C₆₀ fullerene and 100 He atoms functioning as reservoir in a periodical cubic with a side length of 160 Å, subject to the experimental conditions for carbon cluster growth. We employed the Brenner potential^[38,39] for C–C interactions and Leonard–Jones potential for He–He and C–He interactions. Simulations were performed by velocity Verlet algorithm with a time step of 0.2 fs, and the simulated temperature of the thermal bath (He atoms) ranges from 2000 to 3100 K every 100 K. At every temperature point, simulations were repeated until the deviation of averaged rate constant k_{1st} drops below 1%.

The MD simulations show that Stone–Wales transformation of C₆₀ depends on the rotation of bonds on hexagon–hexagon boundary, i.e., a progress involving two key atoms (the inset of Fig. 3), and thus Eq. (7) in our model should be used. The pseudo reaction coordinate method was employed to scan the potential surface and obtain the corresponding MEP with a barrier, $E_0 = 3.65$ eV. In the classical case of the TST, the prefactor of Eq. (3) was replaced with the Vineyard frequency,^[5,40] i.e.,

$$k_{1st} = \frac{\prod_{i=1}^{3N-6} \nu_{\text{react}}(i)}{\prod_{i=1}^{3N-7} \nu_{\text{TS}}(i)} e^{-E_0/k_B T}. \quad (15)$$

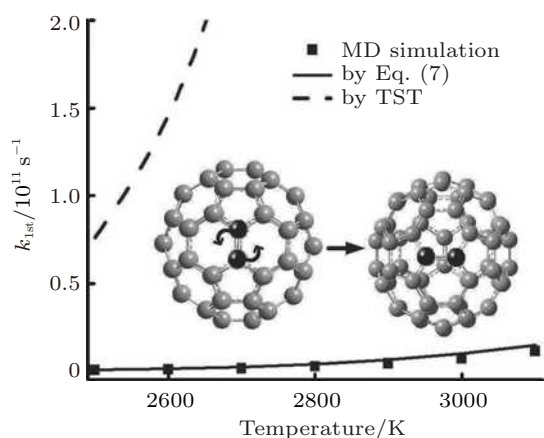


Fig. 3. The rate constant of Stone–Wales transformation of C_{60} , by MD simulation (square dot), our model (solid line), and the TST (dashed line).

The prefactor was calculated with the same Brenner potential as that for the MD simulations. Because of the high symmetry of C_{60} fullerene, there exist 10 identical bond rotation modes of Stone–Wales transformation, and thus the calculated reaction rate should be multiplied by 10 to get the total rate in both our model and the TST. As shown in Fig. 4, the results of MD simulations are in excellent agreement with our model but far away from the results of the TST. For higher temperatures (> 2600 K), the deviation goes beyond about one or two orders of magnitudes. Certainly, other versions of the TST may produce different results, but it is impossible to produce

a rate that is smaller than the one presented in Fig. 3 by one or two orders of magnitudes since in such situation the static potential barrier can be precisely determined via the interaction potential function and no quantum effect takes place in the MD simulations.

Now, we verify the theoretical model in another way. For unimolecular reactions, when the reaction temperature is higher than the Debye temperature, i.e. $T > 200\text{--}400$ K, the result of the TST (Eq. (3)) is reduced to Eq. (15). Given the fact that the exponential part of Eq. (15) is different from Eq. (5) or (7) in our model, equations (15) and (5) (or Eq. (7)) are employed to fit the $k_{1st}\text{--}T$ curves of the Stone–Wales transformation of C_{60} , and especially to fit the experimental $k_{1st}\text{--}T$ curves of the reactions $CH_4 \rightarrow CH_3 + H$, $CH_3OH \rightarrow CH_3 + OH$, and $CF_3CH_2Cl \rightarrow CF_2CHCl + HF$,^[32–34] and we examined if the fitted potential barrier E_f is equal to E_0 , the static potential barrier. In the picture of our model, equation (7) should be applied to the reactions $CH_4 \rightarrow CH_3 + H$ and $CH_3OH \rightarrow CH_3 + OH$ since these bond breakage progresses involve two key atoms, like the Stone–Wales transformation of C_{60} , while for the dissociation reaction $CF_3CH_2Cl \rightarrow CF_2CHCl + HF$, equation (5) should be applied because the reaction is invoked the vibration mode of H atom (which can be confirmed by the following *ab initio* calculations of reaction path), i.e., a progress involving one key atom. In

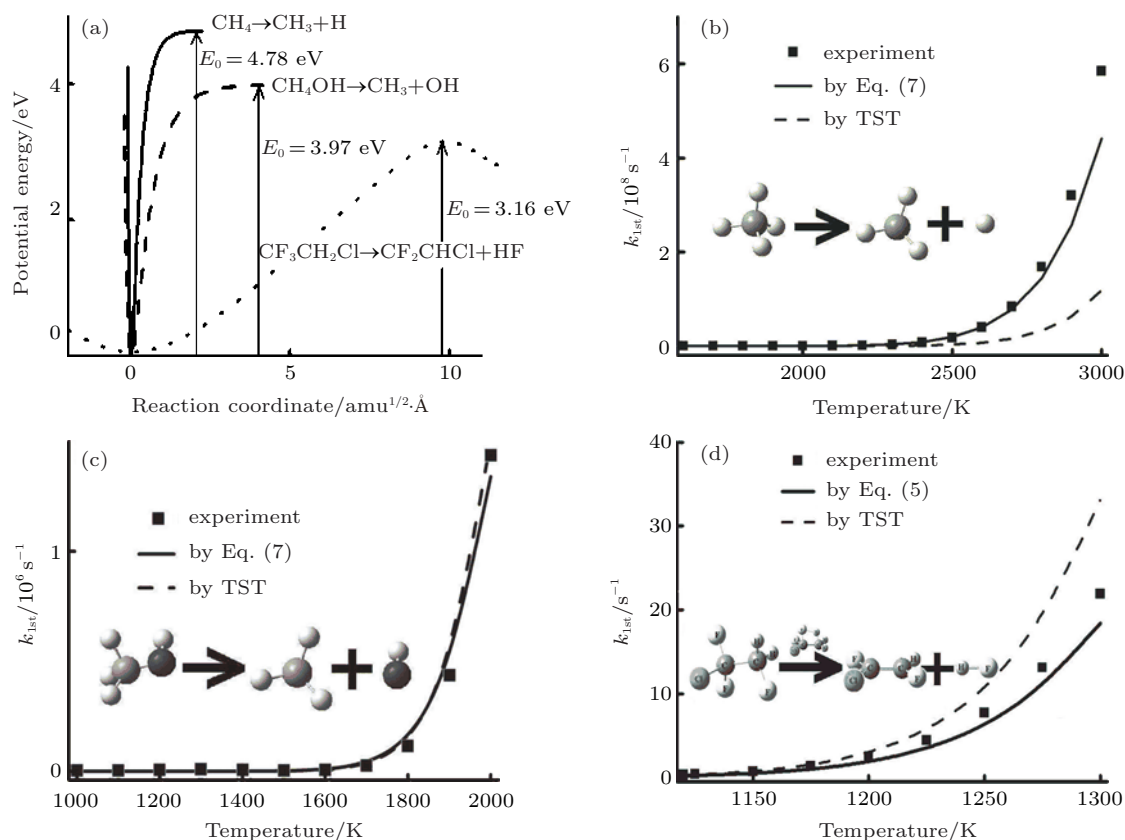


Fig. 4. The MEP of reactions $CH_4 \rightarrow CH_3 + H$, $CH_3OH \rightarrow CH_3 + OH$, and $CF_3CH_2Cl \rightarrow CF_2CHCl + HF$ (a), and the corresponding experiment data, the results of our theory (solid line), and the TST (dashed line), which are shown in (b), (c), and (d), respectively.

terms of the TST, the temperatures of all the three reactions are much higher than the Debye temperature, and therefore equation (15) is applicable to the experimental $k_{1st}-T$ curves. As shown in Table 1, the barriers fitted by our model all get close to the accurate values, while the barriers fitted by

Table 1. The barriers E_0 of C_{60} Stone–Wales transformation and the reactions $CH_4 \rightarrow CH_3 + H$, $CH_3OH \rightarrow CH_3 + OH$, and $CF_3CH_2Cl \rightarrow CF_2CHCl + HF$. The three columns are the accurate reaction barrier E_0 , the barrier E_1 fitted by our model, and E_2 derived by Eq. (15), respectively.

	E_0/eV	E_1/eV	E_2/eV
C_{60} Stone–Wales Transformation	3.65	3.76 ^{a)}	3.49
$CH_4 \rightarrow CH_3 + H$	4.87 ^[35]	4.80 ^{a)}	4.54
$CH_3OH \rightarrow CH_3 + OH$	3.92 ^[36]	3.98 ^{a)}	3.90
$CF_3CH_2Cl \rightarrow CF_2CHCl + HF$	3.17 ^[37]	3.17 ^{b)}	2.93

^{a)}Eq. (7), ^{b)}Eq. (5).

Eq. (15) are all smaller by about 10%, which is exactly the expected value predicted by our model.^[30] Similar deviation was also found in the experimental study of adatom self-diffusion on Cu (100) and Pt (111) surfaces, where the barriers fitted by Eq. (15) are always smaller than the theoretical energy barrier by about 10%.^[1,41]

Finally, our model and the TST were applied on an *ab initio* level via the Gaussian 03 package to calculate the reaction rate of reactions $CH_4 \rightarrow CH_3 + H$, $CH_3OH \rightarrow CH_3 + OH$, and $CF_3CH_2Cl \rightarrow CF_2CHCl + HF$ in the temperature range of the experiments.^[32–34] Specifically, the reaction barriers E_0 , MEPs and canonical frequencies were investigated, and internal rotor modification^[42] was applied for TST calculations. Geometry optimization, the calculation of the MEP and canonical frequencies were performed by the QCISD(T) method^[43] with the cc-pVTZ basic set to reach a high level of accuracy in electronic energy calculation. To avoid possible inaccuracy in the calculation of the static barriers, experimental values of E_0 ^[35–37] were used in both our model and the TST to calculate the rate constants.

The potential energy profiles along the MEP are shown in Fig. 4(a). For $CH_4 \rightarrow CH_3 + H$ and $CH_3OH \rightarrow CH_3 + OH$, the potential energy increases with increasing the length of C–H and C–O bonds. For $CF_3CH_2Cl \rightarrow CF_2CHCl + HF$, the H atom approaches the F atom with increasing potential energy, and then forms an HF molecule with decreasing potential energy, leaving away from the system.

The measured barrier E_0 for the C–H bond cleavage in the reaction $CH_4 \rightarrow CH_3 + H$ is 4.87 eV,^[35] which gets close to the calculation value 4.78 eV. This bond cleavage reaction was attributed to the motion of the H and C atoms departing from each other, i.e., the process involving two key atoms (Eq. (7)). Since there are four independent vibration modes for the bond breaking in CH_4 , the calculated rate were multiplied by 4 both in our theory and the TST. As shown in Fig. 4(b),

our model is in good agreement with experimental data, while the TST yields poor results, although it is qualitatively in accordance with the experimental data. For the dissociation reaction $CH_3OH \rightarrow CH_3 + OH$, the calculated barrier 3.97 eV gets close to the experimental value 3.92 eV.^[36] Reasonably, this bond cleavage reaction also involves two key atoms. For this reaction, our model (Eq. (7)) and the TST are both in good agreement with the experimental data (Fig. 4(c)). For the decomposition reaction $CF_3CH_2Cl \rightarrow CF_2CHCl + HF$, the calculation of MEP shows that the reaction is induced by the scissoring vibration mode of one H atom approaching an F atom. Because the mass of H atoms is much smaller than the molecule, the mass center of the molecule is nearly static in the reaction process, so equation (5) for one-key-atom reaction was applied. The calculated rate should be doubled since there are two independent H–F pairs. Using the experimental barrier 3.17 eV^[37] (while the calculated value is 3.16 eV), it is shown that equation (5) is in better agreement with the experimental data than the TST (see Fig. 4(d)).

4. Application to bimolecular reactions

To test Eq. (8) (or Eq. (9)) and Eq. (10) for bimolecular reactions, we performed MD simulations for the dimerization of C_{60} fullerenes and compare our model with the conventional TST without any quantum effect.^[31] The simulation system was setup by putting two isolated C_{60} molecules in He ambient of about 100 atm at room temperature. On a temperature range of 360–720 K, simulations were performed and repeated until the deviation of averaged reaction rate was below 5% at every temperature point. It was shown that the simulation results are in agreement with our model but very far away from the TST.

Recent provided experiment data for rate constants of the elementary bimolecular reactions $S + SO_2 \rightarrow SO + SO$ ^[44] and $NH_3 + Cl \rightarrow NH_2 + HCl$ ^[45] in gas phase were employed to examine our model. For $S + SO_2 \rightarrow SO + SO$, the *ab initio* calculation at the level of B3LYP showed that the reaction proceeds on the triplet state surface with $E_0 = 0.78$ eV.^[46] On this bases, our model produced rate constants in agreement with the experimental results, while the rate constants from the TST are about one order of magnitude smaller.^[31] For $NH_3 + Cl \rightarrow NH_2 + HCl$, it is notable that the remarkable difference between the two calculations of the TST lies only in the choice of a canonical^[45] or a microcanonical^[46] system, showing some uncertainty existed in the TST. The deviation of the TST for a similar reaction $NH_3 + H \rightarrow NH_2 + H_2$ can be seen in Ref. [47]. In contrast, no artificial factors are included in our model and the calculation of the reaction rate is in good agreement with the experimental measurements.^[31]

5. Summary

In summary, a statistic mechanical model was developed to predict elementary reaction rates without empirical parameters. Compared with the conventional TST, the model is more accurate and works more easily, needing merely the potential curves along a given reaction path, which can be determined via common *ab initio* calculations. It is worth noting that the accurate potential barrier along the reaction path cannot be simply used in the conventional TST to predict the reaction rate, and meanwhile, if the Arrhenius function is employed to fit experimental data, the fitted barrier is not yet the exact static potential barrier, but instead a smaller one. We believe that our model will find wide applications in the near future.

References

- [1] Marinica M C, Barreateau C, Spanjaard D and Desjonqueres M C 2005 *Phys. Rev. B* **72** 115402
- [2] Mei Q S and Lu K 2007 *Prog. Mater. Sci.* **52** 1175
- [3] Celina M, Gillen K T and Assink R A 2005 *Polym. Degrad. Stab.* **90** 395
- [4] Smith I W M 2008 *Chem. Soc. Rev.* **37** 812
- [5] Ala-Nissila T, Ferrando R and Ying S C 2002 *Adv. Phys.* **51** 949
- [6] Eyring H 1935 *J. Chem. Phys.* **3** 107
- [7] Truhlar D and Garrett B 1980 *Acc. Chem. Res.* **13** 440
- [8] Truhlar D G, Garrett B C and Klippenstein S J 1996 *J. Phys. Chem.* **100** 12771
- [9] Quack M and Troe J 1974 *Ber. Bunsen-Ges. Phys. Chem.* **78** 240
- [10] Quack M and Troe J 1975 *Ber. Bunsen-Ges. Phys. Chem.* **79** 170
- [11] Quack M and Troe J 1975 *Ber. Bunsen-Ges. Phys. Chem.* **79** 469
- [12] Georgievskii Y and Klippenstein S J 2005 *J. Chem. Phys.* **122** 194103
- [13] Kohen A, Cannio R, Bartolucci S and Klinman J P 1999 *Nature* **399** 496
- [14] Basran J, Sutcliffe M J and Scrutton N S 1999 *Biochemistry* **38** 3218
- [15] Schreiner P R, Reisenauer H P, Pickard IV F C, Simmonett A C, Allen W D, Mayyus E and Csaszar A G 2008 *Nature* **453** 906
- [16] Zhang X, Datta A, Hrovat D A and Borden W T 2009 *J. Am. Chem. Soc.* **131** 16002
- [17] Miller W H 1974 *Adv. Chem. Phys.* **25** 69
- [18] Miller W H 2001 *J. Phys. Chem.* **105** 2707
- [19] Tromp J W and Miller W H 1986 *J. Phys. Chem.* **90** 3482
- [20] Miller W H, Zhao Y, Ceotto M and Yang S 2003 *J. Chem. Phys.* **119** 1329
- [21] Schubert R, Waalkens H and Wiggins S 2009 *Few-Body Syst.* **45** 203
- [22] Buchowiecki M and Vanicek J 2010 *J. Chem. Phys.* **132** 194106
- [23] Suleimanov Y V, Collepardo-Guevara R and Manolopoulos D E 2011 *J. Chem. Phys.* **134** 044131
- [24] Allen J W, Green W H, Li Y, Guo H and Suleimanov Y V 2013 *J. Chem. Phys.* **138** 221103
- [25] Yongle L, Suleimanov Y V, Yang M, Green W H and Guo H 2013 *J. Phys. Chem. Lett.* **4** 48
- [26] Marcus R A 1952 *J. Chem. Phys.* **20** 359
- [27] Lin Z Z, Yu W F, Wang Y and Ning X J 2011 *Europhys. Lett.* **94** 40002
- [28] Cleri F and Rosato V 1993 *Phys. Rev. B* **48** 22
- [29] Li P and Ning X J 2004 *J. Chem. Phys.* **121** 7701
- [30] Yu W F, Lin Z Z and Ning X J 2013 *Chin. Phys. B* **22** 116802
- [31] Li W Y, Lin Z Z, Xu J J and Ning X J 2012 *Chin. Phys. Lett.* **29** 080501
- [32] Sutherland J W, Su M C and Michael J V 2001 *Int. J. Chem. Kinet.* **33** 669
- [33] Spindler K and Wagner H G 1982 *Ber. Bunsenges. Phys. Chem.* **86** 2
- [34] Millward G E and Tschuikow-Roux E 1972 *Int. J. Chem. Kinet.* **4** 559
- [35] Heneghan S P, Knoot P A and Benson S W 1981 *Int. J. Chem. Kinet.* **13** 677
- [36] Jasper A W, Klippenstein S J, Harding L B and Ruscic B 2007 *J. Phys. Chem. A* **111** 3932
- [37] Enstice E C, Duncan J R, Setser D W and Holmes B E 2011 *J. Phys. Chem. A* **115** 1054
- [38] Brenner D W 1990 *Phys. Rev. B* **42** 9458
- [39] Halicioglu T 1991 *Chem. Phys. Lett.* **179** 159
- [40] Vineyard G H 1957 *J. Phys. Chem. Solids* **3** 121
- [41] Yelon A, Movaghar B and Branz H M 1992 *Phys. Rev. B* **46** 12244
- [42] Ayala P Y and Schlegel H B 1998 *J. Chem. Phys.* **108** 2314
- [43] Pople J A, Head-Gordon M and Raghavachari K 1987 *J. Chem. Phys.* **87** 5968
- [44] Murakami Y, Onishi S, Kobayashi T, Fujii N, Isshiki N, Tsuchiya K, Tezaki A and Matsui H 2003 *J. Phys. Chem. A* **107** 10996
- [45] Gao Y D, Alecu I M, Hsieh P C, Morgan B P, Marshall P and Krasnoperov L N 2006 *J. Phys. Chem. A* **110** 6844
- [46] Xu Z F and Lin M C 2007 *J. Phys. Chem. A* **111** 584
- [47] Ju L P, Han K L and Zhang J Z H 2008 *J. Comput. Chem.* **30** 305